



ISSN: 2723-9535

Available online at www.HighTechJournal.org

HighTech and Innovation Journal

Vol. 3, No. 2, June, 2022



Analysis of Vertically Oriented Coupled Shear Wall Interconnected with Coupling Beams

Vikram Singh^{1*}, Keshav Sangle¹

¹ Structural Engineering Department, Veermata Jijabai Technological Institute, Mumbai, India.

Received 12 January 2022; Revised 23 April 2022; Accepted 11 May 2022; Available online 24 May 2022

Abstract

The nonlinear static response of a vertically oriented coupled wall subjected to horizontal loading is presented in this research article. The 3 storey vertically oriented coupled wall interconnected with coupling beams is modelled as solid elements in a finite element (FE) software named Abaqus CAE and the steel reinforcement is modelled as a wire element. For simulation of concrete models, a concrete damaged plasticity constitutive model is taken into consideration in this research. Moreover, with the help of concrete damage plasticity parameters, validation of two rectangular planar walls was executed with an error of less than 10 percent. Finally, these parameters are used for modeling and analyzing the static behavior of coupled walls connected with coupling beams. Furthermore, the maximum unidirectional horizontal loading helped in obtaining the compression and tensile damage as well as scalar stiffness degradation. Significantly, the research also found the plastic hinge location in the coupled wall as well as in the coupling beam, which are of utmost importance in nonlinear analysis.

Keywords: Nonlinear Analysis; Concrete Damaged Plasticity Model; Plastic Hinge Formation.

1. Introduction

In buildings, the lateral mechanisms that are most commonly used are RC-coupled walls with a set of interconnected coupling beams. Beams are mainly reinforced conventionally or diagonally for coupling with the walls. While designing mid-to high-rise buildings, managing the lateral displacement of a building subjected to earthquake loading is a prevailing issue. This lateral displacement has been thought to be a primary indication of the degree of damage induced to the system and, if not managed, can also contribute to unintentional contact between structures (i.e., pounding). Performance criteria are generally displacement-based in the performance-based design approach. Quality requirements in the approach to performance-based design are typically based on displacement. Firstly, keeping this displacement within an acceptable limit ensures the main purpose of planning to have sufficient strength and stiffness. In multi-storey commercial and residential structures, coupled walls are a typical type of shear wall. Through a fusion of the coupling beam's frame action and the wall pier's flexural action, a coupled shear wall system resists lateral forces. By the shear accumulation in the coupling beam, an axial force coupled is formed. Shear stress and geometrical limits have directed the use of these 2 types of coupling beams [1, 2] in testing and also in shear failures that are reported in conventional coupling beams in buildings subjected to earthquakes. Coupling beam should be diagonally reinforced if $V_u \geq 4\sqrt{f_c}A_{cw}$ and $(l_n/h) < 2$ i.e. aspect ratio is less than 2, as per ACI 318-14 [3]. And if the aspect ratio is equal or greater than 4 i.e., $l_n/h \geq 4$ then it should be designed as special moment frame beams.

* Corresponding author: er.vikramsingh@outlook.com

<https://dx.doi.org/10.28991/HIJ-2022-03-02-010>

➤ This is an open access article under the CC-BY license (<https://creativecommons.org/licenses/by/4.0/>).

© Authors retain all copyrights.

Anyhow, nominal strength shall be taken less than $10A_{cw}\sqrt{f_c}$. Beam possess capabilities of dissipating energy throughout the height of building, is appropriately designed. It could be seen, however, at the wall's base, the absolute overturning moment (M_o) is resisted by flexural stresses in a traditional manner, while moments and axial forces are resisted in the coupled walls. These comply with the following clear statement of equilibrium.

$$M = M_1 + M_2 + IT \quad (1)$$

During earthquake, the main function of coupling beams is to pass the shear between the coupled walls. In the consideration of coupling beams, it is important to understand that considerably greater inelastic excursions in these beams will occur during an earthquake than in the coupling walls. A higher number of shear reversals as in beams than those in the walls can be anticipated during an earthquake. Designing of many coupling beams with stirrups are carried out as flexural member and allocating concrete little shear resistance. As in diagonal tension failure occurs in these beams. Two triangular members are eventually divided by failure through diagonal crack in comparatively small beams. If only vertical stirrups are able to transfer the shear linked to beam's flexural over-strength on the faces of the wall, diagonal stress loss could occur. Tough to sustain the high bond stresses across the horizontal flexural strengthening during reversed cyclic loading, sufficient to maintain along short span, the high rate of momentary changes. These parallel reinforcements appear to produce stress across the entire span, so that shear is transferred mainly through the beam by a diagonal strut of concrete.

The coupling beams are critical part to the earthquake response of coupled walls, which has an immense effect on the demands of shear and axial force in the coupled walls [4]. Linear analysis was widely used in current practise to achieve sectional demands in favour of the design, and with either analogous static or modal response spectrum. It is well recognized that in the wall piers, the demands of shear force are undervalued by the demands that are determined from linear analysis [2, 5–7]. To account for cracking, the used of formalized element stiffness is the major downgrade of linear analysis. This not only hinders the redistribution principle usage but also results in demand of irrational flexure and shear in coupled walls [4]. During execution of capacity design such irrational demands causes complications. For nonlinear time-history analysis of building performance-based design is required [8]. Euler-Bernoulli beams having uniaxial materials and fibre sections are most common solution for modelling the walls in this case, while the coupling beams being typically modelled using shear springs [9, 10]. It is impossible to compensate for nonlinear flexure-shear interaction, these modelling methods have their own drawbacks. To analyse the behaviour of the coupled wall system [11–15], some experimental as well as analytical research has been performed. However, experiments on RC coupled walls are very minimal compared to various studies on independent planar shear walls [16–20] and coupling beams [21–27].

Previous studies reported the effects of various forms of coupling beams as well as drawn attention towards degrees of coupling that showed the redistribution between wall piers of moment and base shear. Out of all these experimental projects, Lehman et al. [28] done a testing with high-end response as well as damage data on a single planar wall system, which offers useful knowledge for analytical modelling analysis. In order to perform studies of various structures, analytical models with adequate precision, accuracy are now commonly and desperately required in order to facilitate and concentrate on the formation of plastic hinge in the coupled wall as well as in coupling beams. There is still a major gap in the previous research that has been conducted for the analytical modelling of the critical RC coupled wall structure, primarily due to the complex behaviour of coupling beams.

Analysed and simulated a vertically oriented coupled wall with coupling beams under nonlinear regime in computer aided engineering software named Abaqus CAE. The research reported in this paper provides a CDP parameter to actually observe behaviour, damage as well as the formation of plastic hinge zone in coupled wall, which are only predicted previously on rectangular shear wall. The model is indeed a plasticity-based continuum damage model for concrete. Compressive crushing and tensile cracking of the concrete are presumed to be the main failure mechanism which helps in formation of plastic hinge zone.

2. Concrete Damaged Plasticity Model

There have been some holes as well as microcracks in the concrete before sustaining external loads, recognized as "damage". Specifically, the mechanism of failure is triggered via evolution and development of incremental damage at different levels (micro-cracks, hole etc.). Later, nonlinear stress strain properties are primarily caused by cracks. The deterioration of steel often results in plastic deformation, which entails not just to micro-cracks extension and microscopic mechanism defects and furthermore deformation and slipping in conjunction with the material flow. Thus, the sensible constitutive relationship will be the elastic-plastic model of damage that reflects the plastic deformation and the elastic damage, which are 2 different types of a mechanism. To prevent problems in studying the microstructure, an isotropic microstructure is usually regarded in order to explore its deformation and failure mechanism. In accordance with model developed by Lubliner et al., concrete damage plasticity model was created in Abaqus CAE, a finite element software. The above model utilizes isotropic elastic damage models in combination with the compressive plasticity or isotropic tensile for simulating the inelastic behaviour of concrete. Relying on

presumption that, throughout the case of unpredictable loading, like cyclic loading, there will be the similar damage across all directions applicable to the concrete. At the same time, attention is given not just to loss of elastic stiffness due to the compressive & tensile plastic strain, as well to the stiffness recovery during cyclic loading. For describing the material's mechanical properties, elastic model is adopted by CDP model generally in elastic stage. Relationship between the modulus of elasticity in CDP model upon taking further into phase of damage is presented as;

$$E = (1 - d) E_0 \tag{2}$$

where, the modulus of elasticity is indicated by E_0 initially, in compression plastic damage factor d_c or in tension d_t which generally varies from 0 until 1, where 0 denotes materials as undamaged, 1 represents material strength is entirely vanished.

2.1. Cyclic Loading

Over reverse loading, for regulating the restoration of material stiffness, the model uses w_c and w_t underneath the operation of uniaxial vibratory loading.

The schematic illustration of the recovery of E_0 during uniaxial cyclic loading when w_c equals to 1 and w_t equals to 0 are defined as the weighting factors of compression and tension. The concrete's tensile stress grows under the axial tension. Cracking can be observed in concrete in case the stress approaches at point A (peak), however the tensile stiffness may reduce in case loading is applied towards B point, where d_t be able to represented equal to $E = (1 - dt)E_0$. The curve would decrease the effective stiffness $E = (1 - dt)E_0$ by slope, that is, the trajectory BC, when it is unloaded during that moment. Enforcing concrete with reverse axial pressure, it will follow the path CD if w_c equals to 0 and it will follow the route CMF if w_c equals to 1. Unloading and imposing reversed tensile loading takes place, as it hits point F. When the factor of stiffness recovery is 0 or 1, it will follow GH or GJ route respectively.

2.2. Uniaxial Tension/Compression

With respect to concrete's tensile stress-strain curve, the values exceeding limit of elastic part would be included in Abaqus CAE in the form of $\sigma_t - \varepsilon_t^{ck}$. After the deduction of elastic strain of the material from the total strain, we get the tensile cracking strain, as shown in Figure 2.

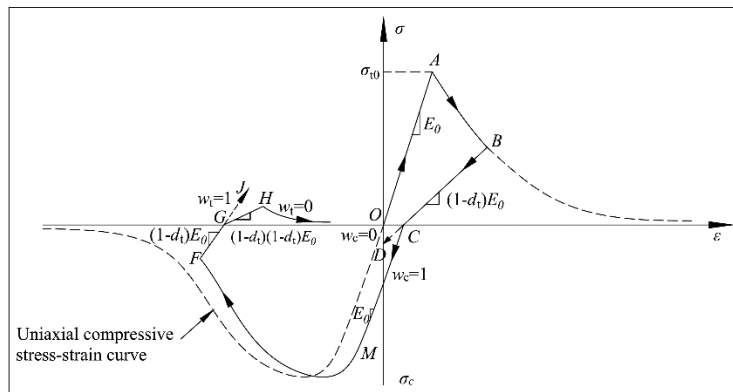


Figure 1. Diagram for stiffness recovery under uniaxial loading

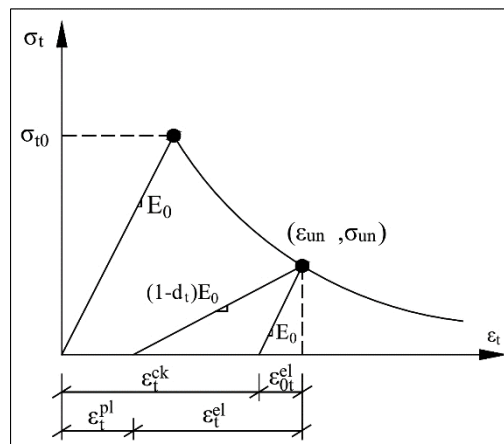


Figure 2. Stress strain curve in tension

In Figure 2, ε_t^{el} and ε_{0t}^{el} show the concrete’s tensile plastic strain is damaged and undamaged, respectively; σ_{un} designate as the stress, ε_{un} as strain of the unloading point; and ε_t^{ck} and ε_t^{pl} indicate the concrete’s cracking and tensile plastic strain, respectively.

In the form $d_t - \varepsilon_t^{ck}$, the tensile damage statistics is entered into Abaqus CAE software. As per the below mentioned equations, the cracking strain would be transformed by the software automatically into plastic strain,

$$\varepsilon_t^{pl} = \varepsilon_t^{ck} - \frac{d_t \sigma_t}{1 - d_t E_0} \tag{3}$$

In case ε_t^{ck} is small or ε_t^{pl} is negative, that implies the tensile unloading path converges, Abaqus CAE will warn as “there will be no tensile damage when $\varepsilon_t^{pl} = \varepsilon_t^{ck}$ ” as an error.

With respect to concrete's compressive stress-strain curve, the values exceeding limit of elastic part would be included in Abaqus CAE in the form of $\sigma_t - \sigma_c^{in}$. After the deduction of elastic strain of the material from the total strain, we get the compressive cracking strain, as shown in Figure 3.

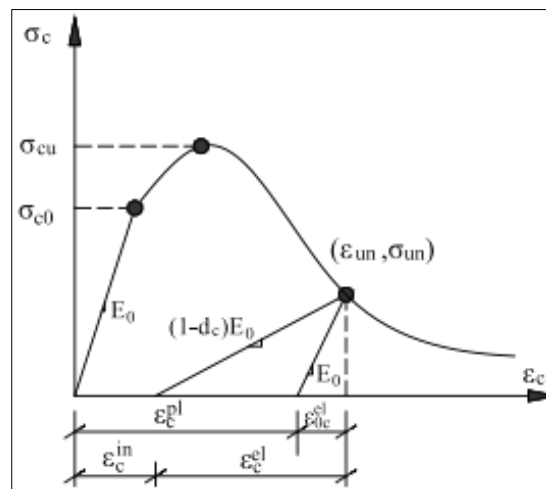


Figure 3. Stress strain curve in compression

In Figure 3, ε_c^{el} and ε_{0c}^{el} , show the concrete’s compressive plastic strain is damaged and undamaged, respectively; σ_{un} designate as the stress, and ε_{un} as strain of the unloading point; and ε_c^{in} and ε_c^{pl} , indicate the concrete’s cracking and compressive plastic strain, respectively.

In the form $d_c - \varepsilon_c^{in}$, the compressive damage statistics is entered into Abaqus CAE software. As per the below mentioned equations, the cracking strain would be transformed by the software automatically into plastic strain,

$$\varepsilon_c^{pl} = \varepsilon_c^{ck} - \frac{d_c \sigma_c}{1 - d_c E_0} \tag{4}$$

In case ε_c^{in} is small or ε_c^{pl} is negative, that implies the compressive unloading path converges, Abaqus CAE will warn as “there will be no compressive damage when $\varepsilon_c^{pl} = \varepsilon_c^{in}$ ” as an error.

3. Validation

3.1. Problem 1 (RW2)

The dimension of the wall tested by Thomsen and Wallace [29] is as shown in Figure 4. Height of the wall being 3660 mm with the thickness of 102 mm having web length of 1220 mm. Material properties used for the purpose of design are $f'c = 27.4$ MPa (4 ksi) and $f_y = 414$ MPa (60 ksi). Hoops spacing of 50 mm centre to centre with special transverse reinforcement. Although the boundary element's volumetric ratio of transverse reinforcement was 0.0132, the tighter spacing was expected closest to the wall boundary delaying the onset of buckling for the two longitudinal bars, resulting in a slightly higher displacement capacity. Because of practical reason, eight vertical bars on the boundary have hoops, with the hoop's spaced at 178 mm from outer boundary. Hence the transverse reinforcement stretched for confining the boundary region beyond the required length of 112 mm.

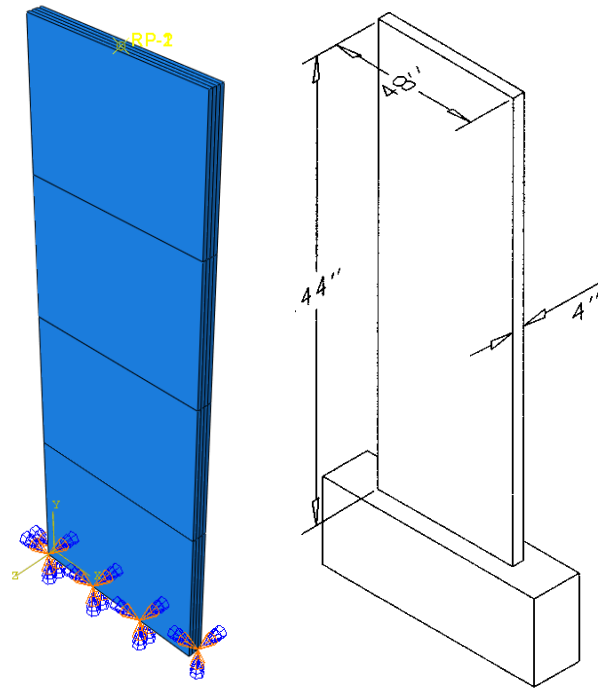


Figure 4. 3-D view of specimen RW1 tested [29] and model simulated [30]

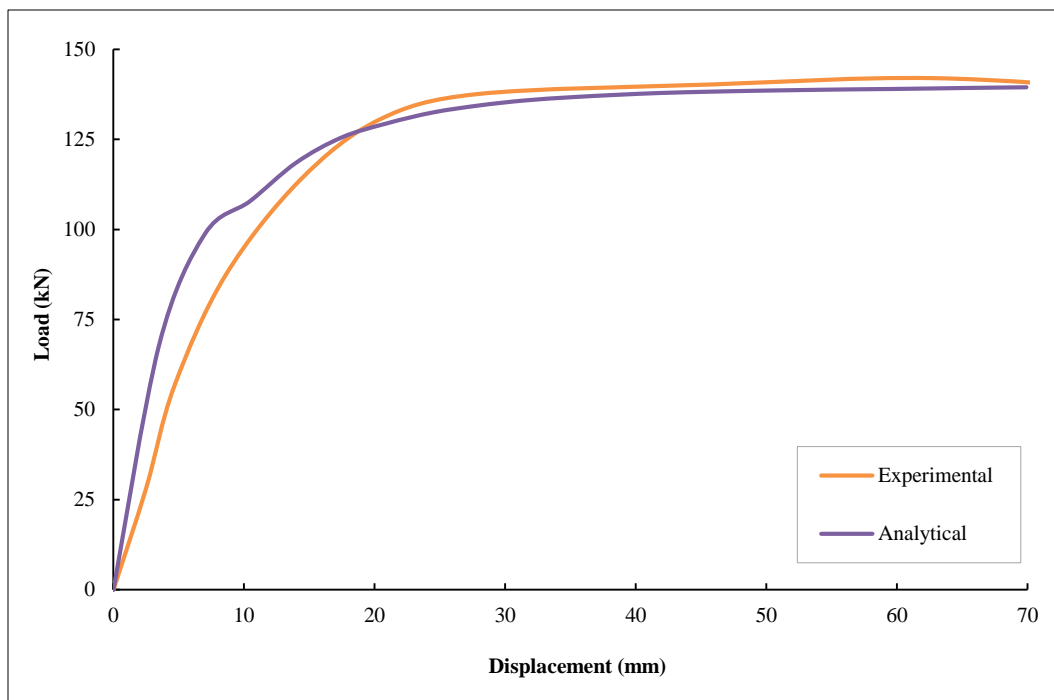


Figure 5. Comparison of pushover curve obtained experimentally and analytically

3.2. Problem 2 (SW21)

Structural shear wall, SW21 is analysed in this paper for validating the nonlinearity procedure to be carried out on coupled shear wall. Lefas et al. [31] carried out experimental investigation on SW21 by exposing it to static incremental loading. Wall was 1300 mm long having 65 mm thickness, also width was 650mm i.e aspect ratio being 2. Top beam on to the wall was 1150 long with cross section of 150 mm x 200 mm. Vertical reinforcement was provided for monolithic behaviour as seen in Figure 6. Bottom beam is fixed having length as 1150mm with cross section of 300x200 mm. Stirrups with horizontal reinforcement are used on the edges for confining the wall. Maximum deformation of 20.61 mm was observed in laboratory by Lefas et al. [31] against the load of 127 kN. Load-displacement comparison of analytical with respect to experimental results are showcased in Figure 7.

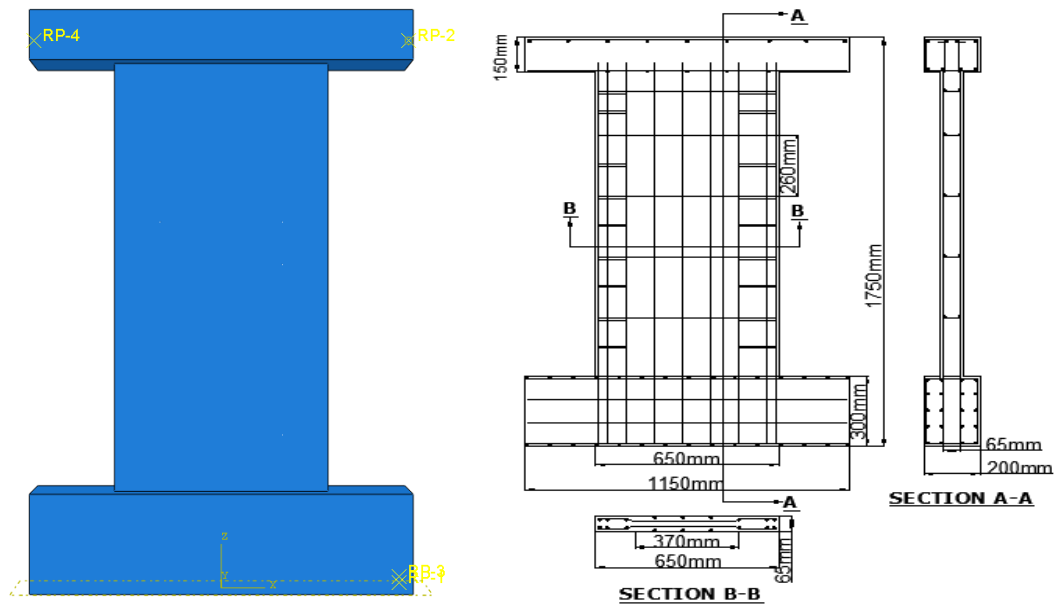


Figure 6. Details of Wall SW21 [31] and model simulated [30]

A parametric investigation is carried out with varying parameters which could clearly depict the behaviour of wall as compared to the experimental behaviour. Wall modelled in FEM software, ABAQUS CAE deformed 19.52 mm against lateral load of 127 kN as seen in Figure 7. Nominal error in results of analytical against experimental shows the perfect agreement. Figure 7 showcases simulation of model from 0 upto 127 kN, same as the response of experimental setup.

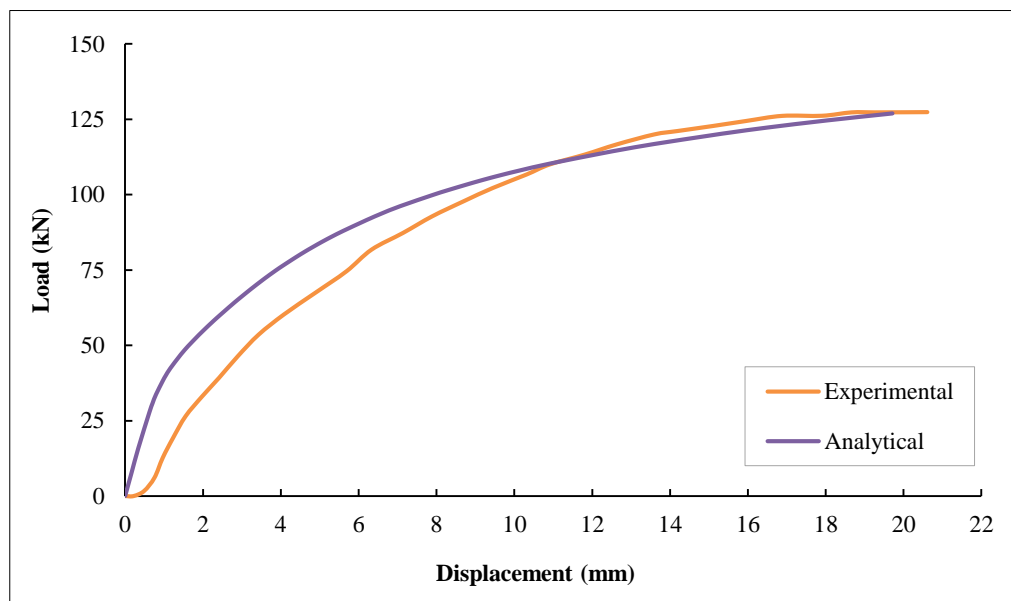


Figure 7. Comparison of load-displacement curve obtained experimentally and analytically

4. Material Models

It is important to provide the material actions as precisely as possible for a realistic FEM, as the correct choice of constitutive models contributes. When performing non-linear finite element analysis, material properties could play a significant role. The materials with different constitutive relationships for getting the appropriate input data are described in this section. Concrete acts in a non-linear way following a small linear part under uniaxial compression. ABAQUS considers elasticity to evaluate the response of the material till the material reaches the specified cracking stress, after which the non-linear behaviour of the material rules. Command of "elastic" with the software is used for defining the material properties. For material behaviour, concrete's modulus of elasticity as well as Poisson's ratio are defined.

For this analysis, as mentioned previously, the Concrete Damaged Plasticity Model was selected. Several distinct commands are used to better describe the CDP. The first of all is the command of "damage plasticity", as discussed earlier in Table 1, which specifies the 5 plastic damage parameters. The parameters used can be seen in the table below.

Table 1. Material Properties of concrete used in concrete damage plasticity model

Material's parameters		Plasticity parameters	
M42.8		Dilation angle	35
Concrete elasticity		Eccentricity	0.1
E (MPa)	29143.3	f_{b0}/f_{c0}	1.16
Poisson's ratio	0.2	K	0.667
Concrete compressive behavior		Viscosity parameter	0.0005
Yield stress (MPa)	Inelastic strain	Damage parameter, C	Inelastic strain
17.1364	0	0	0
25.4685	0.0003	0	0.0003
32.7616	0.00061	0	0.00061
38.3455	0.00091	0	0.00091
41.7251	0.00121	0	0.00121
42.8	0.00151	0	0.00151
41.3744	0.00182	0.03331	0.00182
37.6477	0.00212	0.12038	0.00212
32.69933	0.00242	0.236	0.00242
27.52355	0.00273	0.35693	0.00273
22.74824	0.00303	0.4685	0.00303
18.64458	0.00333	0.56438	0.00333
15.25523	0.00364	0.64357	0.00364
12.51307	0.00394	0.70764	0.00394
10.31453	0.00424	0.75901	0.00424
8.55547	0.00454	0.80011	0.00454
7.14505	0.00485	0.83306	0.00485
6.00901	0.00515	0.8596	0.00515
5.08860	0.00545	0.88111	0.00545
4.33799	0.00576	0.89865	0.00576
3.72167	0.00606	0.91305	0.00606
3.21218	0.00636	0.92495	0.00636
2.78818	0.00667	0.93486	0.00667
2.43305	0.00697	0.94315	0.00697
2.13377	0.00727	0.95015	0.00727
1.88008	0.00757	0.95607	0.00757
Concrete tensile behavior		Concrete tension damage	
Yield stress (MPa)	Cracking strain	Damage parameter, T	Cracking strain
4.28	0	0	0
2.37448	0.00015	0.44522	0.00015
1.68225	0.00029	0.60695	0.00029
1.31732	0.00044	0.69221	0.00044
1.08973	0.00059	0.74539	0.00059
0.93329	0.00073	0.78194	0.00073
0.81867	0.00088	0.80872	0.00088
0.73083	0.00103	0.82924	0.00103
0.66121	0.00117	0.84551	0.00117
0.60457	0.00132	0.85875	0.00132
0.55752	0.00147	0.86974	0.00147
0.51777	0.00162	0.87902	0.00162
0.48372	0.00176	0.88698	0.00176
0.45419	0.00191	0.89388	0.00191
0.42832	0.00206	0.89993	0.00206
0.40545	0.0022	0.90527	0.00220
0.38509	0.00235	0.91003	0.00235
0.36683	0.00250	0.91429	0.00250
0.35035	0.00264	0.91814	0.00264
0.33540	0.00279	0.92163	0.00279

5. Finite Element Modelling and Analysis

Previously, the reinforced concrete shear wall was modelled and validated using Abaqus software with concrete damaged plasticity parameters. Later, using same parameters, the modelling and analysis of coupled shear wall was carried out as it is most commonly executed wall in construction. Also, very less research is involved specially in nonlinear state. Displacement based method is used as the focus of study to observe the plastic hinge formation in coupling beams and wall.

The height of coupled shear wall is 9000 mm with a thickness of 230 mm. The slabs are provided at top and bottom of the wall. Dimensions of upper slab and bottom slab are 2860×286×200 mm and 2860×286×300 mm respectively. Upper slab is used for the application of the load and bottom slab is used as a foundation to provide fixity to wall. The doubly reinforced coupling beam is provided at each floor level of 3000 mm. The beam is reinforced with 2-16 bars provided at both top and bottom side of the beam. Two legged 8mm stirrups are provided at 150 mm centre to centre spacing. The solid model and reinforcement model of coupled wall are shown in Figures 8 and 9.

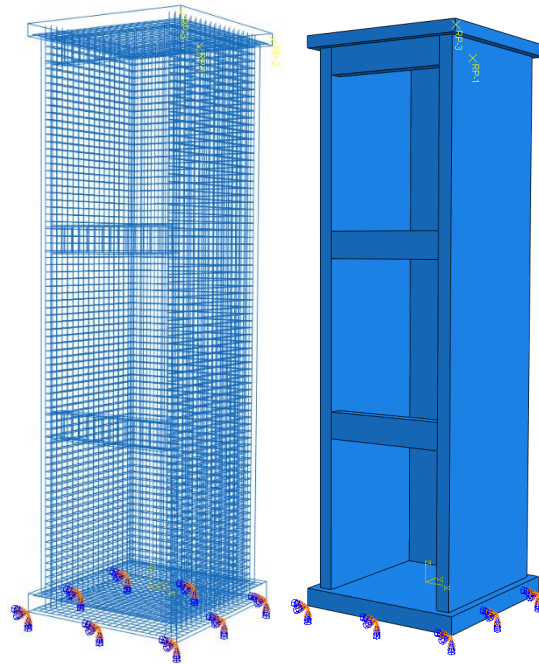


Figure 8. Solid and reinforcement model in finite element (FE) software

Usually, tensile strengthening in concrete structures is produced in Abaqus using rebars, which are 1-D rods which are embedded in master surfaces or as an independent bar. Along with metal plasticity models, rebars are commonly used for describing the material behaviour. Rebars are superposed on standard element type mesh that are used for modelling concrete. Concrete behaviour is regarded individually without rebars using this modelling approach. Effects such as dowel action as well as bond slip in association with concrete-rebar interface, approximate modelling is introduced in modelling of concrete by tension stiffening for simulating load transfer through rebars along cracks. In complicated situations, modelling a rebar may be cumbersome, but also crucial if not performed correctly as it may allow failure in analysis because of the absence of reinforcement in important regions.

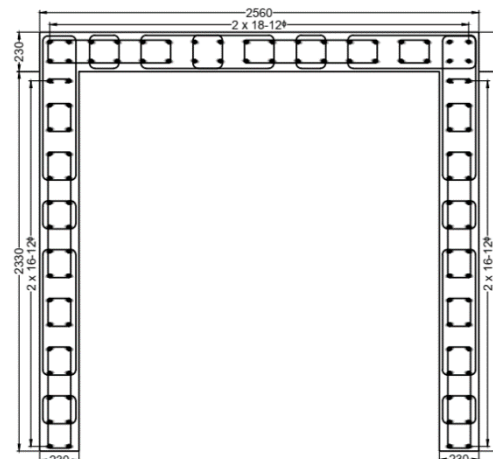


Figure 9. Cross-sectional reinforcement detailing of vertically oriented coupled shear wall

6. Results

Analysis of coupled wall model was performed for investigating the behaviour of wall as well as of coupling beams. As described below some general observations were triggered from the nonlinear behaviour of the model. Reinforced coupled wall connected with coupling beams had great influence on the overall behaviour of the model subjected to lateral loads. As soon as the crushing of concrete occurred, wall developed flexure-dominant behaviour, ductile with yielding of reinforcement dissipating a high rate of energy. On the wall concrete panel, flexural-tension cracks as well as shear inclined cracks had steadily progressed till the peak lateral load was attained. Coupling beams stimulated the failure, as wall were designed to develop plastic hinge for model subjected to horizontal loads.

A full connection was established between reinforcement and concrete by using embedded command in Abaqus CAE. On the contact, there was no visible separation between concrete and reinforcement. Reinforcement, upper and lower slab were detailed and designed for bearing the horizontal loads till the failure is achieved. Near the contact area of the top surface of foundation and the vertical walls where wall transfer the load from wall to foundation, small horizontal crack could be seen. As a result, the most relevant features of the analytical behaviour are emphasized based on the analysed data.

6.1. Stiffness Analysis

Stiffness degradation occurs when in-plane lateral loads cause significant stress and damage to the walls. As a result of this stress and damage, the stiffness (K) of the walls gradually diminishes. The ratio between the peak lateral load (P) and its corresponding total drift was used to determine the lateral stiffness (K). The traditional reinforced concrete wall was found to have the most significant stiffness deterioration. Stiffness degradation leads to crack in concrete. Specially in the coupled shear wall linked with coupling beams but still can be better controlled by embedding vertical reinforcement in the edges of wall. Pushover curve is generated in Abaqus CAE for coupled wall as presented in Figure 10.

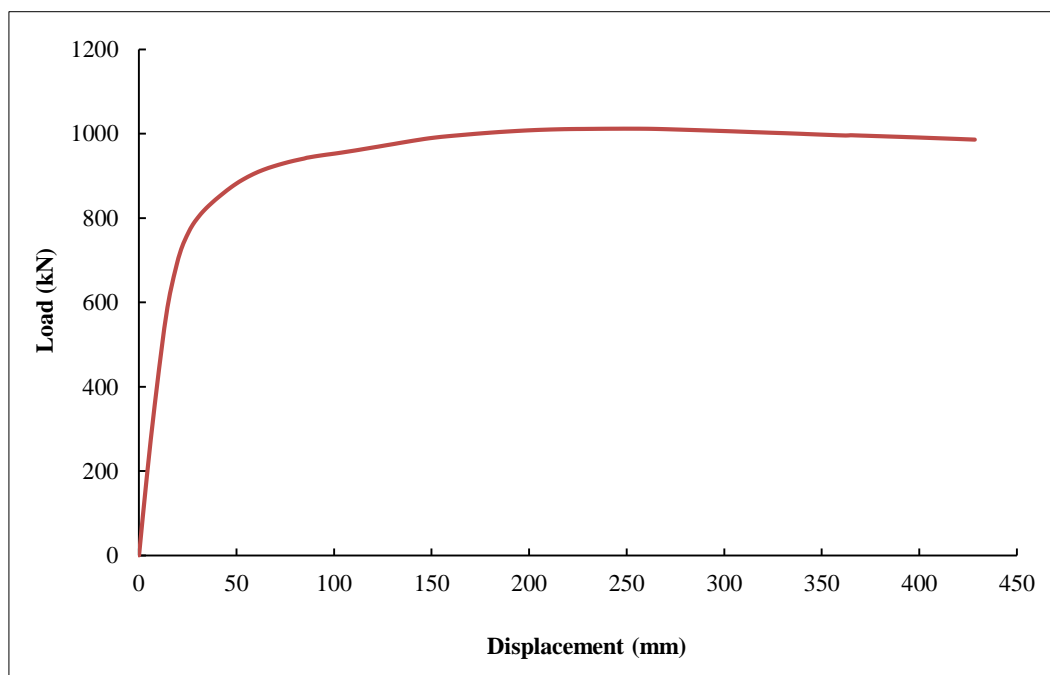


Figure 10. Pushover curve of coupled shear wall system

6.2. Stress and strain

In the instance stresses were generally observed at the base of the slab foundation and on vertical reinforcement of the vertically oriented coupled shear wall. Also, the edges of coupling beams connecting the wall exhibits stresses. Evolution of compression damage (DAMAGEC) is shown in Figure 11.

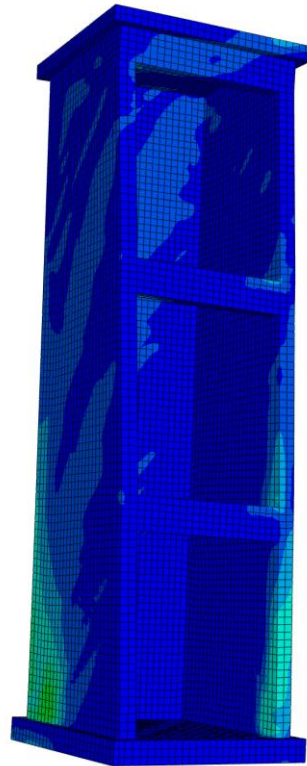


Figure 11. Evolution of compression damage

6.3. Failure Mode

The model's state at the time of failure is depicted in Figure 12. The most significant structural components, all of which were damaged during the failure, were the vertically oriented wall as well as the coupling beams. The inclined shear cracks that developed along the edges of the coupling beams caused these modes. The brittle failure modes developed in the coupling beams that were subjected to the shear force. As shown by Subedi [32], shear load reversals crushed coupling beams on the edges and at the base of the vertically oriented coupled wall.

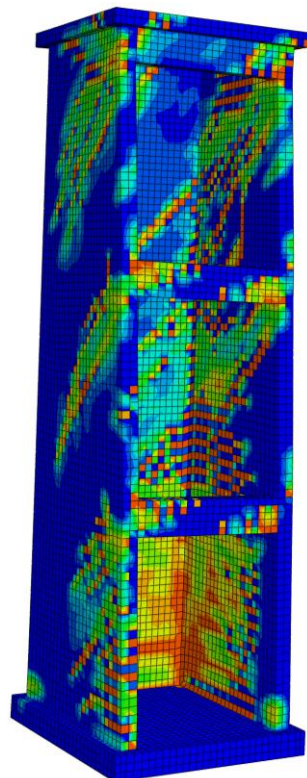


Figure 12. Scalar stiffness degradation (SDEG)

6.4. Occurrence of Plastic Hinges

Plastic hinges developed on the coupled wall with coupling beams in the same way that they did in the validated model. The walls formed plastic hinges at the edge of the coupling beams, followed by the base of the walls. At the ends of the coupling beams, plastic hinges were discovered, and at the base of the wall, more plastic hinges developed. Concrete crushing was also observed in zones of maximum compression and enhanced deformation development under constant loads.

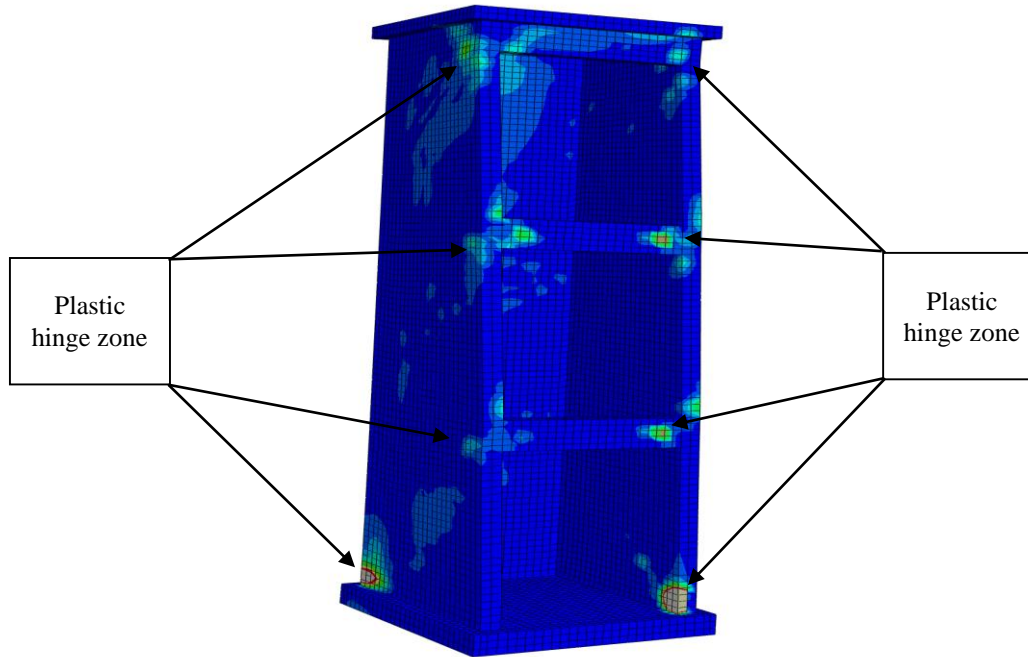


Figure 13. Formation of plastic hinges in wall and coupling beam

7. Conclusions

The purpose of this paper was to investigate the nonlinear behaviour of concrete coupled shear walls with coupling beams under lateral loads. Model behaviour and materials components, with regards to ductility, maximum load, as well as stiffness degradation, were discussed to observe the performance of the model. At the very same time, the damage, failure modes, and progression of cracks were showcased using the analytical procedure. Until the formation of plastic hinges, their behavior is highlighted in different stages.

Following conclusions can be drawn:

- Openings in the wall above and below coupling beams caused torsional effects on the coupled wall. Low dissipative behaviour of horizontally oriented coupling beams affected the ductility level and shear governed failure of coupling beams led to a reduction in ductility. It is suggested to improve the ductility of vertically oriented coupled shear walls that have large openings.
- High degradation of lateral stiffness and a high state of stress were recorded for the model. A viable solution is embedding reinforcement at the edge of vertical walls. This increases the axial stiffness for suppressing severe cracks in concrete, as well as the overall lateral stiffness.
- Diagonal tension cracks triggered the coupling beam's brittle failure mode, which was reinforced with horizontal reinforcement and vertical stirrups. Shear force reversal caused crushing of concrete at the edge of beams.

8. Declarations

8.1. Author Contributions

Conceptualization, V.S. and K.S.; methodology, V.S.; software, V.S.; validation, V.S.; formal analysis, V.S.; investigation, V.S.; resources, V.S.; data curation, V.S.; writing—original draft preparation, V.S.; writing—review and editing, K.S.; visualization, K.S.; supervision, K.S.; project administration, K.S. All authors have read and agreed to the published version of the manuscript.

8.2. Data Availability Statement

The data presented in this study are available in the article.

8.3. Funding

The authors received no financial support for the research, authorship, and/or publication of this article.

8.4. Declaration of Competing Interest

The authors declare that they have no known competing financial interests or personal relationships that could have appeared to influence the work reported in this paper.

9. References

- [1] Santhakumar, A. R. (1974). Ductility of coupled shear walls. PhD thesis, University of Canterbury, Christchurch 8041, New Zealand.
- [2] Fischinger, M. (Ed.). (2014). Performance-Based Seismic Engineering: Vision for an Earthquake Resilient Society. Geotechnical, Geological and Earthquake Engineering. doi:10.1007/978-94-017-8875-5.
- [3] A.C.I. Committee, 318-14 (2019). Building Code Requirements for Structural Concrete and Commentary. Farmington Hills: American Concrete Institute. doi:10.14359/51716937.
- [4] Alvarez, R., Restrepo, J. I., Panagiotou, M., & Santhakumar, A. R. (2019). Nonlinear cyclic Truss Model for analysis of reinforced concrete coupled structural walls. *Bulletin of Earthquake Engineering*, 17(12), 6419–6436. doi:10.1007/s10518-019-00639-8.
- [5] Panagiotou, M., Restrepo, J. I., & Conte, J. P. (2011). Shake-Table Test of a Full-Scale 7-Story Building Slice. Phase I: Rectangular Wall. *Journal of Structural Engineering*, 137(6), 691–704. doi:10.1061/(asce)st.1943-541x.0000332.
- [6] Panagiotou, M., & Restrepo, J. I. (2011). Displacement-Based Method of Analysis for Regular Reinforced-Concrete Wall Buildings: Application to a Full-Scale 7-Story Building Slice Tested at UC–San Diego. *Journal of Structural Engineering*, 137(6), 677–690. doi:10.1061/(asce)st.1943-541x.0000333.
- [7] Panagiotou, M., & Restrepo, J. I. (2009). Dual-plastic hinge design concept for reducing higher-mode effects on high-rise cantilever wall buildings. *Earthquake Engineering and Structural Dynamics*, 38(12), 1359–1380. doi:10.1002/eqe.905.
- [8] NIST. (2017). Guidelines for nonlinear structural analysis and design of buildings. Part I - general. In NIST GCR 17-917-46v1 (p. 137). doi:10.6028/NIST.GCR.17-917-46v1.
- [9] ASCE 41-13. (2014). Seismic Evaluation and Retrofit of Existing Buildings. American Society of Civil Engineers. doi:10.1061/9780784412855.
- [10] Naish, D., Fry, A., Klemencic, R., & Wallace, J. (2013). Reinforced concrete coupling beams-part II: Modeling. *ACI Structural Journal*, 110(6), 1067–1075. doi:10.14359/51686161.
- [11] Zhang, P. (2013). Nonlinear dynamic analysis model for RC shear wall. *Applied Mechanics and Materials*, 275–277, 1020–1023. doi:10.4028/www.scientific.net/AMM.275-277.1020.
- [12] Mazars, J., Kotronis, P., & Davenne, L. (2002). A new modelling strategy for the behavior of shear walls under dynamic loading. *Earthquake Engineering and Structural Dynamics*, 31(4), 937–954. doi:10.1002/eqe.131.
- [13] Sholeh, M., Braam, C. R., Hordijk, D. A. & Van Keulen, D.C. (2014). Investigation into behaviour of coupled shear walls by means of continuous method. Master thesis, Technical university of Delft, Delft, Netherlands.
- [14] Honarparast, S., & Chaallal, O. (2019). Non-linear time history analysis of reinforced concrete coupled shear walls: Comparison of old design, modern design and retrofitted with externally bonded CFRP composites. *Engineering Structures*, 185, 353–365. doi:10.1016/j.engstruct.2019.01.113.
- [15] Ding, R., Tao, M. X., Nie, X., & Mo, Y. L. (2018). Analytical model for seismic simulation of reinforced concrete coupled shear walls. *Engineering Structures*, 168, 819–837. doi:10.1016/j.engstruct.2018.05.003.
- [16] Lu, X., Xie, L., Guan, H., Huang, Y., & Lu, X. (2015). A shear wall element for nonlinear seismic analysis of super-tall buildings using OpenSees. *Finite Elements in Analysis and Design*, 98, 14–25. doi:10.1016/j.finel.2015.01.006.
- [17] Turgeon, J. (2011). The seismic performance of coupled reinforced concrete walls. PhD Thesis, University of Washington, Washington, United States. Available online: <https://digital.lib.washington.edu/researchworks/handle/1773/17060> (accessed on February 2022).
- [18] Abdullah, S. A., & Wallace, J. W. (2019). Drift capacity of reinforced concrete structural walls with special boundary elements. *ACI Structural Journal*, 116(1), 183–194. doi:10.14359/51710864.
- [19] Abdullah, S. A. Reinforced Concrete Structural Walls: Test Database and Modeling Parameters. University of California.

- [20] Almeida, J. P., Tarquini, D., & Beyer, K. (2016). Modelling Approaches for Inelastic Behaviour of RC Walls: Multi-level Assessment and Dependability of Results. *Archives of Computational Methods in Engineering*, 23(1), 69–100. doi:10.1007/s11831-014-9131-y.
- [21] Eom, T. S., Park, H. G., & Kang, S. M. (2009). Energy-based cyclic force-displacement relationship for reinforced concrete short coupling beams. *Engineering Structures*, 31(9), 2020–2031. doi:10.1016/j.engstruct.2009.03.008.
- [22] Yang, C., Chen, S.-C., Yen, C.-H., & Hung, C.-C. (2022). Behaviour and detailing of coupling beams with high-strength materials. *Journal of Building Engineering*, 47, 103843. doi:10.1016/j.jobbe.2021.103843.
- [23] Li, G. Q., Pang, M., Sun, F., Jiang, J., & Hu, D. (2018). Seismic behavior of coupled shear wall structures with various concrete and steel coupling beams. *Structural Design of Tall and Special Buildings*, 27(1), 1405. doi:10.1002/tal.1405.
- [24] Mihaylov, B. I., & Franssen, R. (2017). Shear-flexure interaction in the critical sections of short coupling beams. *Engineering Structures*, 152, 370–380. doi:10.1016/j.engstruct.2017.09.024.
- [25] Seo, S. Y., Yun, H. Do, & Chun, Y. S. (2017). Hysteretic Behavior of Conventionally Reinforced Concrete Coupling Beams in Reinforced Concrete Coupled Shear Wall. *International Journal of Concrete Structures and Materials*, 11(4), 599–616. doi:10.1007/s40069-017-0221-8.
- [26] Wang, T., Shang, Q., Wang, X., Li, J., & Kong, Z. (2018). Experimental validation of RC shear wall structures with hybrid coupling beams. *Soil Dynamics and Earthquake Engineering*, 111, 14–30. doi:10.1016/j.soildyn.2018.04.021.
- [27] Álvarez, R., Restrepo, J. I., Panagiotou, M., & Godínez, S. E. (2020). Analysis of reinforced concrete coupled structural walls via the Beam-Truss Model. *Engineering Structures*, 220, 111005. doi:10.1016/j.engstruct.2020.111005.
- [28] Lehman, D. E., Turgeon, J. A., Birely, A. C., Hart, C. R., Marley, K. P., Kuchma, D. A., & Lowes, L. N. (2013). Seismic Behavior of a Modern Concrete Coupled Wall. *Journal of Structural Engineering*, 139(8), 1371–1381. doi:10.1061/(asce)st.1943-541x.0000853.
- [29] Thomsen, J. H., & Wallace, J. W. (2004). Displacement-Based Design of Slender Reinforced Concrete Structural Walls—Experimental Verification. *Journal of Structural Engineering*, 130(4), 618–630. doi:10.1061/(asce)0733-9445(2004)130:4(618).
- [30] ABAQUS (2014). CAE User Guide: ABAQUS Version 6.14. Groupe Dassault, Paris, France.
- [31] Lefas, I. D., Kotsovos, M. D., & Ambraseys, N. N. (1990). Behavior of reinforced concrete structural walls. Strength, deformation characteristics, and failure mechanism. *ACI Structural Journal*, 87(1), 23–31. doi:10.14359/2911.
- [32] Subedi, N. K. (1991). RC - Coupled Shear Wall Structures. I: Analysis of Coupling Beams. *Journal of Structural Engineering*, 117(3), 667 – 680. doi:10.1061/(asce)0733-9445(1991)117:3(667).